JOURNAL OF MATERIALS SCIENCE 28 (1993) 1685–1688

The effect of compatibilizers on the morphology of isotactic polypropylene/linear low-density polyethylene blends

V. FLARIS*, A. WASIAK, W. WENIG‡
Laboratory of Applied Physics, University of Duisburg, 4100 Duisburg, Germany

The morphology of isotactic polypropylene (iPP)/linear low-density polyethylene (LLDPE) blends, compatibilized with ethylene–propylene block copolymer (EP) and two types of styrene–ethylene/butylene–styrene triblock copolymer (SEBS), one containing maleic anhydride, the other no reactive sites, has been investigated by using small-angle X-ray scattering by evaluating their interface distribution functions. To characterize the crystallization behaviour of the blends, their spherulitic growth rates have been measured under the polarizing microscope and nucleation and crystallization kinetics data have been evaluated. The addition of LLDPE to iPP alone has a pronounced effect on the lamellar morphology of the iPP. Adding compatibilizer to the iPP/LLDPE blend leads to a further decrease of the lamellar thickness. Concurrently the nucleation density increases while the Avrami exponent drops from $n \sim 2.3$ for iPP to $n = 0.74$ for the iPP/LLDPE/SEBS blend. It is concluded that the compatibilizer causes the polyethylene component to become more highly dispersed in the polypropylene matrix.

1. Introduction

It is known that polypropylene, when melt-blended with polyethylene, increases its impact resistance, while other mechanical parameters, like Young's modulus, decrease [1]. These disadvantages can be, in part, overcome by the introduction of compatibilizers. Compatibilizers commonly used are block copolymers, graft copolymers or chemically reactive polymers [2–5]. It is believed that compatibilizers act on the interface between matrix and modifier, thus influencing the phase morphology [2].

In this work we investigated the system of isotactic polypropylene (iPP) modified with linear low-density polyethylene (LLDPE). Two different copolymers were added as compatibilizers. Crystallization kinetic parameters were measured and the supermolecular morphology was determined employing the new method of the interface distribution function [6, 7].

2. Experimental procedure

2.1. Materials and blend preparation

The starting materials used were isotactic polypropylene (iPP, $\rho = 0.905\ g\,cm^{-3}$), linear low-density polyethylene (LLDPE, $\rho = 0.919\ g\,cm^{-3}$) and as compatibilizers, an ethylene–propylene block copolymer (EP, $\rho = 0.902\ g\,cm^{-3}$, Sample 3) and two grades of a styrene–ethylene/butylene styrene triblock copolymers, SEBS: SEBS 1 (Sample 4), $\rho = 0.899\ g\,cm^{-3}$, and SEBS 2 (Sample 5), $\rho = 0.926\ g\,cm^{-3}$. SEBS 1 contains reactive sites while SEBS 2 does not contain maleic anhydride. All these polymers are standard commercial grade materials with typical additives present. The compositions of the blends prepared are listed in Table I.

The materials were melt blended in a 1.5 in (~ 3.8 cm) Johns single-screw extruder. The conditions used were described in detail previously [8].

2.2. Nucleation kinetics measurements

For observations under the optical microscope (Leitz Metallux II), the samples were pressed to a thickness of approximately 60 μm and placed between microscope slides and put in a Mettler hot-stage. They were then heated to 200 °C for 5 min and then cooled down

TABLE I Blend compositions

Blend	Composition (%)			
	iPP	LLDPE	C_x	x
1	100	0	0	–
2	80	20	0	–
3	72	18	10	EP
4	72	18	10	SEBS 1
5	72	18	10	SEBS 2
6	0	100	0	–

* *Permanent address:* Mechanical Engineering Department, University of Melbourne, Parkville, Victoria, 3052, Australia.
‡Author to whom all correspondence should be addressed.

0022–2461

to a chosen crystallization temperature, T_c. Crossed polarizers were used and the crystallization was monitored on a video screen and recorded on tape. From the video recording, the growth of the spherulites as well as the number of nuclei as a function of time was determined. The crystallization temperatures for the isothermal crystallization were chosen between 120 and 139 °C. Each crystallization experiment was carried out five times at different locations on the sample to allow for error analysis. It was found that both the spherulitic growth rate and the number of nuclei as a function of time could be measured with great accuracy.

2.3. Small-angle X-ray experiments

Small-angle X-ray scattering curves were recorded using a Kratky compact camera. The setting of the camera was such that sufficiently high resolution was ensured (entrance slit width = 30 μm, detector slit width = 75 μm, distance sample–detector slit = 22 cm).

The measurements were controlled by a computer and the temperature of the cooling water was kept constant through a constant-temperature unit. CuK_α radiation was used and monochromatization was achieved through the use of a nickel-filter in conjunction with pulse-height analysis.

Each curve was recorded several times in an angular range corresponding to 0.7×10^{-3} Å $\leqslant s \leqslant 40 \times 10^{-3}$ Å ($s = 2\sin\Theta/\lambda$, 2Θ being the scattering angle and λ the X-ray wavelength). Wide-angle X-ray curves were recorded using a Philips PW 1380 goniometer.

2.4. Polymer characterization

The materials were characterized using differential scanning calorimetry (DSC) and gel permeation chromatography (GPC) to determine the melting temperatures and the molecular weight distributions, respectively. These results are summarized in Table II. The testing conditions were described in detail previously [8, 9].

2.5. Impact testing

Samples for the Charpy impact test were prepared by injection moulding. These were tested on a temperature-controlled Hounsfield impact tester at a temperature of − 20 °C. For a more detailed description, see [8].

TABLE II Polymer characterization data

Material	T_m (°C)	M_n	M_w/M_n
PP	166.4	57 000	5.14
LLDPE	122.5	30 300	3.7
EP	166.8	52 400	5.65
SEBS 1	–	42 400	1.09
SEBS 2	–		

3. Results and discussion

Interface distribution functions [6] were evaluated from the experimentally measured small-angle X-ray scattering curves using the method described earlier [7].

The (one-dimensional) intensity $I(s)$ is the Fourier transform of the square of the self-convolution of the electron density distribution, ρ, and proportional to the Fourier transform of the square of the second derivative of the one-dimensional correlation function, $P(r)$ [10–12]

$$I(s) = F(\Delta\rho^{*2}) \sim F\left(\frac{\partial^2}{\partial r^2}\right)P(r) \quad (1)$$

Ruland [6] showed that

$$\frac{\partial^2}{\partial r^2}P(r) = -\frac{2k_p}{l_p}\delta(r) + g_1(r) \quad (2)$$

where k_p and l_p are constants proportional to the Porod constant and the average chord length [13, 14] respectively, and $g_1(r)$ is the interface distribution function. Equation 1 then becomes

$$I(s) \sim \frac{2k_p}{l_p} - F[g_1(r)] \quad (3)$$

$F[g_1(r)]$ is the interference function, $G_1(r)$, which can be determined from the measured intensity [7]

$$G_1(s) = \frac{16\pi^2 t}{v}[C - D\exp(-As^2) - Is^n] \quad (4)$$

C, D and A are parameters determined by fitting a function proportional to the gas-scattering curve of the equivalent system without interparticle interference [7].

The inverse linear Fourier transform of $G_1(s)$ yields the interface distribution function:

$$g_1(r) = \int_0 G_1(s)\cos(2\pi rs)\,ds \quad (5)$$

The calculated interface distribution functions for all investigated samples are displayed in Fig. 1. A number of maxima and minima are seen which reflect the distances of interfaces in the system. Considering the crystallinities of the samples, the respective maxima at lower distances, r, have to be assigned to the phase with the lower volume fraction. For crystallinities higher than 50% the maxima at low r have to be assigned to the interlamellar distances, while the maxima at higher r values represent the lamellar thicknesses. In our case, however, the volume crystallinity is for almost all samples around 50%, which means that the maxima for lamellar thickness and interlamellar distance overlap. The interface distribution functions therefore have to be interpreted with great care. The distances derived from the positions of the maxima and minima are listed in Table III. We see that iPP and LLDPE exhibit almost the same supermolecular morphology: from the distances d_1 and L (linear) crystallinities of 49.3% for iPP and 50.6% for LLDPE are computed, in both systems the lamellar thickness and the interlamellar distance amounts to ~7 nm. In both samples a second morphology becomes visible with distances (d_2) of 12.4 nm (iPP) and

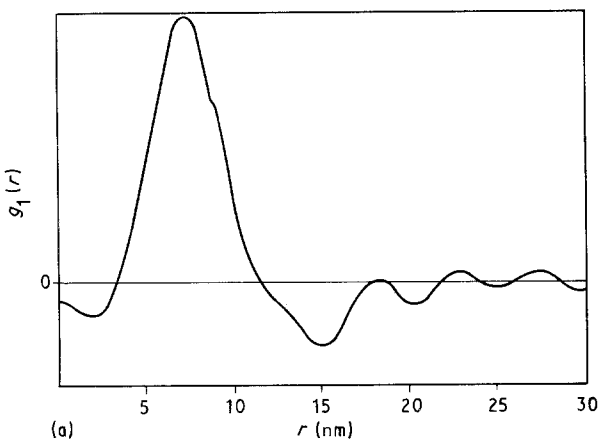

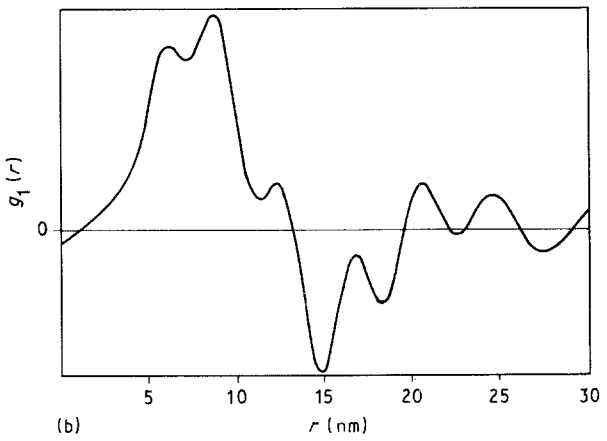

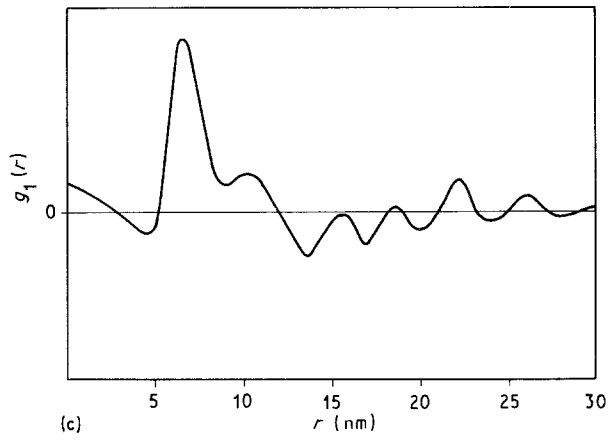

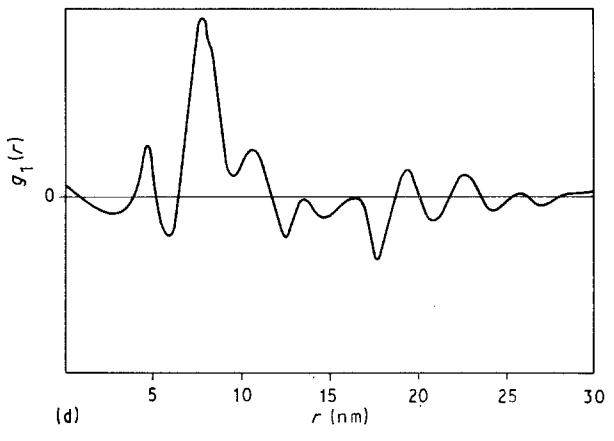

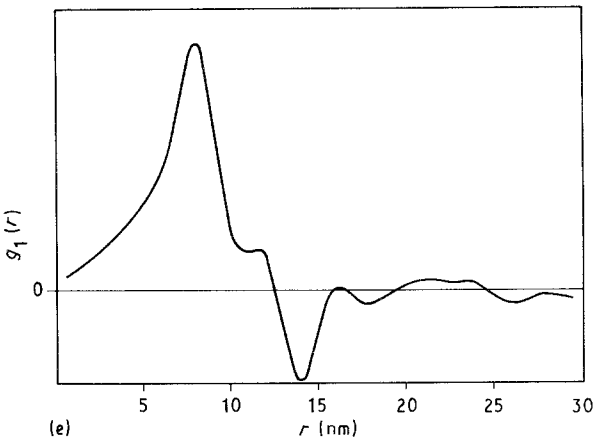

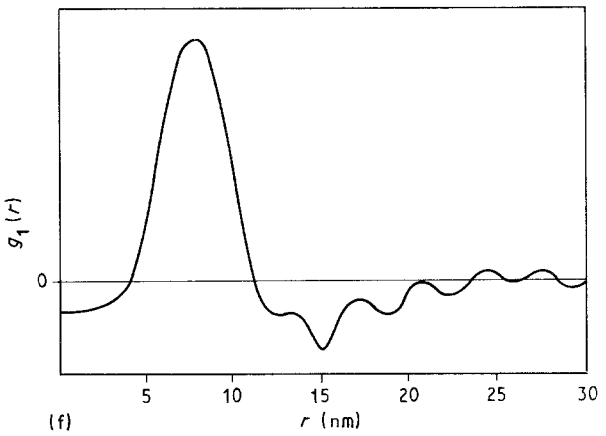

Figure 1 Interface distribution functions of the investigated samples: (a) iPP (Sample 1), (b) 80% iPP + 20% LLDPE (Sample 2), (c) 72% iPP + 18% LLDPE + 10% EP (Sample 3), (d) 72% iPP + 18% LLDPE + 10% SEBS 1 (Sample 4), (e) 72% iPP + 18% LLDPE + 10% SEBS 2 (Sample 5), (f) LLDPE (Sample 6)

TABLE III Results from interface distribution function calculations

Sample	Interface distances (nm)		
	d_1	d_2	L
1			14.8
	7.3	(12.4)	(20.1)
2	5.8		14.6
	8.3	12.1	18.2
3			13.5
	6.65	10.2	16.8
4	4.7		12.5
	7.8	10.8	15.1
5	7.7	(11.8)	14.6
6	7.6	(13.1)	15.0

13.1 nm (LLDPE). These contributions are, however, very weak. In iPP this morphology could probably be attributed to the β-type crystal modification, but it is more likely, that the cooling process during the preparation of the samples is responsible for this contribution.

While both iPP and LLDPE exhibit fairly identical morphologies, the addition of LLDPE to iPP causes a blend morphology which cannot be attributed to any one of the components. The maximum of the interface distribution function at ~7 nm splits up into two maxima at 5.8 and 8.3 nm with long periods at

TABLE IV Results from nucleation and crystallization kinetics measurements

Sample	Nucleation density at 408 K ($M\ mm^{-3}$)	Maximum growth rate, G_{max} (10^{-2} mm s^{-1})	Interfacial free energy, $\sigma\sigma_e$ (10^2 erg^2 cm^{-4})	Avrami exponent, n
1	375	33	12.7	2.3
2	542	49	14.9	2.2
3	1005	60	12.2	2.1
4	517	64	12.4	0.7
5	408	52	12.1	2.2

14.8 and 18.2 nm. These values correspond to a lamellar thickness $d_c = 5.8$ nm and two amorphous distances $d_a = 8.3$ and 12.1 nm. With the given values of the long periods we find linear crystallinities of 39.7% and 11.5%. We see, that the blending of iPP and LLDPE has a pronounced effect on the lamellar morphology. We found similar morphologies for the compatibilized blends: except for Sample 5 (iPP + LLDPE + SEBS2) three maxima and two minima (long periods) occur in the interface distribution function with Sample 4 exhibiting the lowest lamellar thickness. It is interesting to note that this sample gave the best impact result. The Charpy impact value increases from 0.8 kJ m^{-2} (iPP) to 1.2 kJ m^{-2}. For Sample 2 it increases further to 1.3 kJ m^{-2} for Sample 3 and to 2.9 kJ m^{-2} for Sample 4.

It should be expected that such a change of the morphology should be accompanied by a change of the crystallization kinetics.

A survey of the measured parameters for nucleation and crystallization kinetics is given in Table IV. The methods for determining these parameters follow the procedures described in detail earlier [15]. We see that in the blends the nucleation density is higher than in neat iPP. An especially pronounced effect on the nucleation density is visible in the compatibilized blends showing the highest values for the samples containing EP. This behaviour is probably connected with the change of interface morphology, which should affect the nucleation kinetics. Small changes of the interfacial free energy, observed for these samples (cf. Table IV) seem to support the conclusion that additional nucleation sites arise from interfaces due to the blending.

Table IV also shows that the maximum growth rates in the blends substantially increase compared to the values for neat iPP. This effect is especially pronounced in those blends, where compatibilizer is present. The highest value for G_{max} is observed for Sample 4 (which contains SEBS 1, a polymer with reactive sites). The interfacial free energy of the iPP crystal surfaces, determined from the temperature dependence of the growth rate, shows only slight variations with composition. Only for Sample 2, the iPP/LLDPE blend, did we find a slightly higher value. No kind of correlation between $\sigma\sigma_e$ and the growth rate was found, which was expected because the major contribution to $\sigma\sigma_e$ emerges from the lateral crystal surfaces during spherulitic growth.

The values for the Avrami exponent depend only slightly on blend composition by varying from $n \sim 2.3$ for neat polypropylene to $n \sim 2.1$ for Sample 3. Only for Sample 4 (containing SEBS 1) did n drop to the unusual value $n \sim 0.7$. The low values for the Avrami exponent determined in all samples are probably due to two-dimensional growth of the spherulites being confined to the small volume of the thin samples crystallized between the microscope slides [16]. Another reason for the decrease of the Avrami exponent may be the effect of heterogeneous nucleation caused by polymer–polymer interfaces introduced by the blending. The maximum decrease, however, that can be expected due to this reason, cannot exceed the value $n = 1$. It is, therefore, quite probable that the added compatibilizer affects the morphology of the blend by altering the dispersion of the LLDPE component in the iPP matrix prior to the crystallization. As a result of this enhanced dispersion, steric hindrances may be induced causing unidimensional (linear) growth of crystals. Such a type of growth, together with heterogeneous nucleation, may very well be the reason for the observed drop in the Avrami exponent.

References

1. C. B. BUCKNALL, "Toughened Plastics" (Applied Science, London, 1977).
2. W. M. BARENTSEN and D. HEIKENS, *Polymer* **14** (1973) 579.
3. S. ENDO, K. MIN, J. L. WHITE and T. KYU, *Polym. Engng Sci.* **26** (1986) 45.
4. F. IDE and A. HASEGAWA, *J. Appl. Polym. Sci.* **18** (1974) 963.
5. M. YOSHIDA, J. J. MA, K. MIN, J. L. WHITE and R. P. QUIRK, *Polym. Engng Sci.* **30** (1990) 30.
6. W. RULAND, *Colloid Polym. Sci.* **255** (1977) 417.
7. H. W. FIEDEL and W. WENIG, *ibid.* **267** (1989) 389.
8. V. FLARIS and Z. H. STACHURSKI, *J. Appl. Polym. Sci.* in press.
9. *Idem, Polymer Int.* in press.
10. C. G. VONK and G. KORTLEVE, *Koll. Z. Z. Polym.* **220** (1967) 19.
11. *Idem, ibid.* **225** (1968) 124.
12. C. G. VONK, *J. Appl. Crystallogr.* **6** (1973) 81.
13. W. RULAND, *ibid.* **4** (1971) 70.
14. R. PERRET and W. RULAND, *Koll. Z. Z. Polym.* **247** (1971) 835.
15. W. WENIG, H. W. FIEDEL and A. SCHOLL, *Colloid Polym. Sci.* **528** (1990) 528.
16. N. BILLON and J. M. HAUDIN, *ibid.* **267** (1989) 1064.

Received 23 June
and accepted 24 July 1992